

# Modeling the radiative characteristics of airborne mineral aerosols at infrared wavelengths

Irina N. Sokolik and Owen B. Toon

Atmospheric and Oceanic Sciences Department and Laboratory for Atmospheric and Space Physics,  
University of Colorado at Boulder

Robert W. Bergstrom

Bay Area Environmental Research Institute, San Francisco, California

**Abstract.** We explore the importance of the composition of airborne mineral aerosols for assessments of their direct radiative forcing at infrared wavelengths. Our calculations employing Mie theory and data on spectral refractive indices show that the existing variations in refractive indices can cause large changes in the major aerosol optical characteristics. Calculations of IR radiative forcings at the top of the atmosphere and IR downward and upward fluxes, based on an one-dimensional radiation transfer code, give a wide range of results for varying optical models of the mineral aerosols. We estimate that for a “low dust loading” scenario the changes in IR downward flux at the surface relative to dust free conditions are in the range from 7 to 14  $\text{W/m}^2$  depending upon the mineral aerosol selected. Under “dry tropics” atmospheric conditions the IR forcing at the top of the atmosphere is in the range from 2 to 7  $\text{W/m}^2$ . In turn, for a “high dust loading” scenario the calculated changes, relative to dust free conditions, in IR downward flux at the surface vary from 50 to 80  $\text{W/m}^2$ , and the IR forcing at the top of the atmosphere varies from 15 to 25  $\text{W/m}^2$ . Therefore, we conclude that incorporation of regionally and temporally varying dust mineralogical composition into general circulation models could be beneficial for decreasing the currently large uncertainties in the assessment of radiative forcing by the natural and anthropogenic components of the airborne mineral aerosols. Also the use of appropriate mineralogical data is required for remote sensing of the atmospheric aerosols using satellite infrared observations.

## 1. Introduction

An improvement in assessments of global forcing by mineral aerosols requires better modeling of the regional direct radiative forcings at both solar and infrared wavelengths. Several recent papers have focused on estimation of the direct solar forcing by natural and anthropogenic components of the mineral aerosols on regional and global scales [Sokolik and Toon, 1996a, b; Tegen *et al.*, 1996]. It has been pointed out that there are large uncertainties in the assessments of both solar and infrared forcings so that even the sign of net (solar + infrared) forcing remains unclear.

It is recognized that the magnitude of dust IR radiative effects depends on various factors: optical properties, particle size distribution, dust vertical profile, cloud presence, and atmospheric characteristics, among others [Carlson and Benjamin, 1980; Sokolik and Golitsyn, 1993; Tegen *et al.*, 1996]. In this paper we will explore the importance of spatially and temporally varying composition of the airborne mineral aerosols for assessments of their direct radiative forcing at infrared wavelengths. This issue is currently overlooked in dust optical models and in climate studies (see for instance, WCP-55 [1983] and D’Almeida *et al.* [1991]). Our goal is to estimate the range of

the IR radiative forcing which could be caused by varying the regional dust composition. We perform this estimate by employing a model of dust regional optical and radiative properties as well as empirical data.

## 2. Regional Dust Optical Constants and Dust Composition

The airborne mineral aerosol is a mixture of various constituents, the abundance of which could vary depending on the place of origin and dust mobilization processes. Some major aerosol components are quartz, clays (mainly illite, kaolin, and montmorillonite groups), carbonates (calcite, dolomite) and sulfates (gypsum). Also, some amount of organic material and soot could be present, especially in soil-derived (nondesert) aerosols. Each of these constituents has specific features in IR spectra which are the result of lattice vibrations. There is a large body of spectroscopic measurements of IR transmittance and reflectance for various minerals showing the position and intensity of the major absorption bands [Salisbury *et al.*, 1992]. The most intense spectral features of silicates (quartz and clays) in the wavelength range from 8 to 12  $\mu\text{m}$ , where the atmospheric infrared transmission window is found, are due to fundamental asymmetric Si-O-Si stretching vibrations. For instance, quartz has a major band centered at 9.2  $\mu\text{m}$ . In turn, some clays can incorporate Al or other ions as a part of the crystal lattice. In such

Copyright 1998 by the American Geophysical Union.

Paper number 98JD00049  
0148-0227/98/98JD-00049\$09.00

cases Si-O-Al stretching vibrations can result in shifting the band positions and varying the bandwidths. Clay also contains water and hydroxyl in the crystal lattice. Although the fundamental O-H and H-O-H features are commonly seen in the 2-7  $\mu\text{m}$  wavelength region, a variety of significant metal cation-OH bands are found at longer wavelengths. Kaolinite, for instance, has a prominent Al-OH band near 11  $\mu\text{m}$ .

In contrast to silicates, carbonates typically display a strong band near 7  $\mu\text{m}$  due to asymmetric C-O stretching vibrations and weaker bands near 11.4 and 14.3  $\mu\text{m}$ , which can be seen in the spectrum of calcite. In turn, sulfates display a group of intense bands due to the sulfate ions stretching near 8.7  $\mu\text{m}$  and two bending modes near 16  $\mu\text{m}$ , as can be seen in spectra of gypsum.

In the case of a mixture, measurements show that the nature of the IR spectra depends on the abundance of its major constituents [Levin and Lindberg, 1979]. The abundance of major constituents of the airborne mineral aerosol depends on the dust source and upon compositional separation during dust mobilization and transport [Pye, 1987; Gomes and Gillette, 1993]. Therefore, the complex refractive indices and the optical properties would be different for airborne dust originating from different sources. To explore this issue we reexamine available data for refractive indices of airborne dust samples collected at various geographical locations, and then relate them to specific regional dust compositions.

There were some previous attempts to relate refractive indices to dust composition [Patterson, 1981; Sokolik et al., 1993]. In particular, Patterson [1981] intercompared spectral data for the imaginary part of the refractive index of crustal aerosols collected at several geographical locations. He showed that the similarities and differences in the measured values could be understood in terms of mineralogical characteristics of the aerosols. However, no assessment of changes in dust optical and radiative properties due to the differences in refractive indices was done in that study.

A summary of available data on refractive indices is presented in Table 1. Table 1 shows a descriptive name for each refractive index, the wavelength range in which the real,  $n$ , and imaginary,  $k$ , parts have been measured, and the location where dust samples have been collected. As one can see from Table 1, there are no published data for dust which originated in China, India, the Arabian Peninsula, or Australia, which are important contributors to total atmospheric dust loading. There are two spectra of  $n$  and

$k$  of dust from the Sahara desert both measured by Volz [Volz 1973; Fouquart et al., 1987] employing a transmission technique in which dust is suspended in a KBr pellet. Refractive indices of dust from the Negev desert have been measured by Fisher [1976] for background and dust storm conditions using a thin film transmission technique. The data for dust originating in the Afghanistan-Tadzhikistan region have been measured by employing reflectance of pressed dust samples and the Kramers-Kronig theory. The dust samples collected in the southwest part of the United States have been analyzed by Patterson [1981] using a KBr technique similar to that used by Volz [1973]. Only data on the imaginary part have been published. Therefore, we performed calculations of the real part using dispersion analysis. In contrast to the desert dust samples discussed above, so called "dust-like" samples represent soil-derived aerosols of nondesert origin. They have been collected from precipitation over Germany by Volz [1972] and have been used for measurements of the refractive indices by the KBr technique. This set of refractive indices is widely used for modeling dust optical properties for climate studies [e.g., D'Almeida et al., 1991].

The real and imaginary parts of the refractive index summarized in Table 1 are compared in Figures 1a and 1b. Figure 1 presents a larger body of data, than presented by Patterson [1981] and Sokolik et al. [1993], as well as the real part of refractive index.

The observed variations among the data sets presented in Figure 1 could be due to both the differences in measurement techniques and the differences in dust composition. Detailed analysis of measurement techniques by Sokolik et al. [1993] showed that the discrepancies in refractive indices can only partially be explained by the differences in measurement techniques, in spite of many existing technical problems related to the measurement and retrieval procedures. Furthermore, some refractive indices in Figure 1 have been measured with the same technique, which implies that differences are due to mineralogical composition.

Unfortunately, there is no way to quantitatively relate measured refractive indices of the dust samples given in Table 1 to the mineralogical composition because the composition has not been reported. Lack of compositional reports is a major obstacle in obtaining a more useful set of refractive indices for atmospheric aerosols. Instead, we can explain some spectral features of the refractive indices by utilizing independent studies of the mineralogical composition of airborne mineral aerosols which originated from the geographical locations at which the dust

**Table 1.** Refractive Indices in the IR Region of the Airborne Mineral Aerosols Collected at Various Geographical Locations

Nickname	Wavelengths, $\mu\text{m}$	Locations	References
"Sahara dust- Barbados"	2.5-40	Barbados, West Indies	Volz [1973]
"Sahara dust-Niger"	4-40	Niamey, Niger	Volz cited in the work by Fouquart et al. [1987]
"Negev dust" "Clean" "Dust storm"	7.5-12	Negev desert, Israel for background atmospheric conditions for dust storm	Fisher [1976]
"Afghan dust"	2.5-25	Afghanistan -Tadzhikistan	Sokolik et al. [1993]
"Southwest USA dust"	1-16	Whitehill, Texas, United States	Patterson [1981]
"Dust-like"	2.5-40	Germany	Volz [1972]

There were no data reported for China, India, Arabian Peninsula, and Australia.

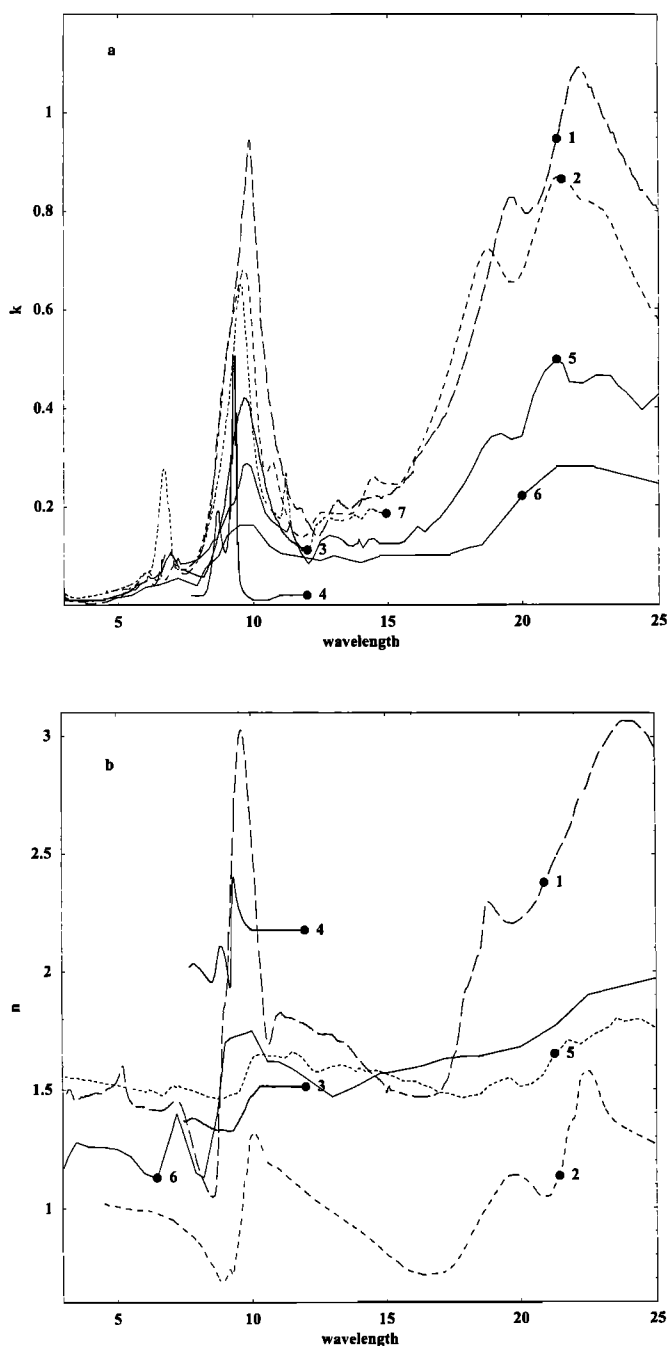


**Figure 1.** The (a) imaginary and (b) real parts of the refractive indices of dust samples summarized in Table 1: curve 1 is for “Sahara dust-Barbados”; curve 2 is for “Sahara dust-Niger”; curves 3 and 4 are for “Negev dust” for “clear” and “dust storm” conditions, respectively; curve 5 is for “Afghan dust”; curve 6 is for “dust-like”; and curve 7 is for “southwest USA dust”.

samples given in Table 1 have been collected. For instance, the peak near  $\lambda = 7 \mu\text{m}$  in the spectrum of  $k$  for the “southwest USA dust” sample is due to presence of calcite. According to the measurements by *Gomes and Gillette* [1993] the mineral aerosol collected over this region has a higher calcite/clay ratio than the dust samples collected over the north Sahara and Afghanistan-Tadzhikistan regions. Indeed the spectra of  $k$  for dust from these two locations show much lower values of  $k$  around  $\lambda = 7 \mu\text{m}$ ,

although weak bands are still present. The variations of the maximum of the imaginary part of refractive index and its position in the 8–12  $\mu\text{m}$  wavelength region may be due to different proportions of major clays and quartz. As was pointed out by *Patterson* [1981], the spectrum for the “southwest USA dust” samples, which have a relatively small amount of quartz, shows a peak which is very similar to that for illite and montmorillonite. In turn, refractive indices for the Negev desert have a narrower peak in the 8–12  $\mu\text{m}$  wavelength region for dust collected during a dust storm than for dust collected under background conditions. The background samples have refractive indices which are similar to those of clays, while the dust storm samples have refractive indices which are similar to those of quartz. Likewise, the composition measurements show the dominance of quartz relative to clays in the accumulation mode of airborne mineral aerosols during dust storms [*Pye*, 1987].

The dominance of quartz also results in large values of the real part of the refractive index (see Figure 1b). The data for  $n$  in Figure 1b for samples which are expected to have larger content of clays have a rather smooth spectrum. Some samples show an anomalous dispersion in  $n$  similar to that of quartz. Dust samples of nondesert origin (“dust-like”) could be influenced by nonsilicate components, since they show only weak silicate features.

Thus overviewing the available optical constants for the various desert dust samples summarized in Table 1, one can make several important generalizations. The available data are rather poor in quality, since the measurement techniques used to obtain refractive indices are poorly justified, since the dust samples are not related to composition, and since they are limited in terms of representation of various dust sources. The refractive indices in Table 1 were measured for dust samples under specific atmospheric conditions after specific transformations during their transport from the dust source to the place where they were collected. Therefore, these optical constants are not adequate for the purpose of modeling the time- and space-varying aerosol optical properties. Finally, due to nonlinear dependencies of aerosol optical properties on the refractive indices, it remains a question if refractive indices measured as an average for a mixture are appropriate to use for modeling of the mineral aerosols optical characteristics [*Bergstrom*, 1973].

Another way to proceed with modeling of dust IR optical properties is to start with the refractive indices of major dust constituents instead of using refractive indices of a dust mixture. Table 2 summarizes some available data on refractive indices at IR wavelengths of major constituents of the airborne mineral aerosols. If the time-dependent size distributions were available for individual constituents, one could calculate optical characteristics of each constituent, and then calculate optical properties of their mixture. Such a procedure would allow us to adequately model optical properties accounting for the varying composition of dust depending on its place of origin as well as its life cycle.

There are some advantages and disadvantages of this approach. Some advantages are that refractive indices for individual minerals are better measured; mixing the optical properties of minerals is more likely to yield correct optical properties than using the optical constants for a mixture of minerals; and the refractive indices may be better related to specific size modes. Also, modeling the individual minerals has the potential to improve our understanding of dust particle shapes. There are some tendencies for given minerals to show specific shapes of particles [*Parungo et al.*, 1995].

The main disadvantage of the above approach is that there are not enough data on regional and global scales to quantify the

**Table 2.** Refractive Indices of Major Constituents of the Airborne Mineral Aerosols at Infrared Wavelengths

Constituents	Wavelengths, $\mu\text{m}$	References
Quartz		
Amorphous form	7.14-50.0	<i>Popova et al.</i> [1972]
	7.14-25.0	<i>Steyer et al.</i> [1974]
Crystalline form	0.736-36.0	<i>Peterson and Weinman</i> [1969]
Montmorillonite	5.0-40.0	<i>Toon et al.</i> [1977]
	2.5-200	<i>Querry</i> [1987]
Illite	2.5-200	<i>Querry</i> [1987]
Kaolinite	5-25	<i>Roush et al.</i> [1991]
Calcite		
Amorphous form	2-32.8	<i>Querry et al.</i> [1978]
Crystalline form	2.5-300	<i>Long et al.</i> [1993]
Gypsum, crystalline form	2.5-300	<i>Long et al.</i> [1993]
Hematite	8.3-50.0	<i>Popova et al.</i> [1973]

size-resolved composition of airborne dust aerosols. Although there is a large body of data on mineralogical composition of the parent soils, it is not an easy task to interpret it in terms of the related composition of the airborne dust, because dust composition also depends on the mobilization processes, which currently are poorly modeled (see further discussions in section 5). Obviously, more studies are necessary to develop quantitative relations between refractive indices and dust composition for various dust sources.

### 3. Computations of Dust Optical Properties at Infrared Wavelengths

By employing Mie theory and data on spectral refractive indices, we calculate dust extinction and absorption coefficients, single scattering albedos, and asymmetry parameters at high spectral resolution to examine differences in these dust optical properties due to varying refractive indices.

To perform Mie calculations, information on particle size distribution is necessary. We examined reported measurements of dust size distributions to select some representative models. There are several major problems in selection of dust particle size distributions. Extensive measurements of dust size distributions published in the literature reveal a large variety of possible particle size spectra. For instance, size distributions can have one or several modes, and particle concentrations can vary by several orders of magnitude across the size distribution. For the purposes of this paper, we modeled dust size distributions with a lognormal function having a median radius in the range from 0.25 to 0.7  $\mu\text{m}$ , which represents the long-lived, distant-transport accumulation mode of airborne dust [Patterson and Gillette, 1977]. The measurements of refractive indices have been performed for samples with particle sizes typically smaller than a few micrometers. However, close to the dust sources a coarse mode, with sizes larger than a few micrometers, can dominate the dust optical properties. We will illustrate this point later on.

Figures 2a - 2c present calculated extinction coefficients,  $K_{\text{ext}}$ , single scattering albedos,  $\omega_0$ , and asymmetry factors,  $g$ , for

various complex refractive indices shown in Figure 1. We assumed a lognormal size distribution with  $r_0 = 0.5 \mu\text{m}$  and  $\sigma = 2$ . The spectra for  $K_{\text{ext}}$  ( $\text{km}^{-1}$ ) are normalized to a particle concentration  $N = 1 \text{ cm}^{-3}$ . Since optical characteristics were calculated for the same size distribution, the differences between the various curves in Figure 2 are due to varying refractive indices. For example,  $K_{\text{ext}}$  for the refractive indices considered can vary by almost a factor of 2 in the 8-12  $\mu\text{m}$  wavelength region. Such a discrepancy in  $K_{\text{ext}}$  is equivalent to an uncertainty in total optical depth due to an error of a factor of 2 in dust loading.

Figures 2b and 2c gives spectra of single scattering albedo and asymmetry factor. In the  $\lambda = 8-12 \mu\text{m}$  wavelength region,  $\omega_0$  varies from 0.1 to 0.94. Higher values of  $\omega_0$  are due to higher values of the real part of the refractive indices. Increases in  $n$  cause increases in scattering coefficient, and therefore result in higher values of single scattering albedo. Such high values of  $\omega_0$  indicate that scattering by dust can not be ignored in simulating IR radiation transfer.

It is known that optical properties of the airborne mineral aerosols depend on both refractive indices and dust particle size distribution. Figures 3a and 3b depict spectra of  $K_{\text{ext}}$  and  $\omega_0$  calculated for an accumulation mode of dust particles having a log-normal size distribution with  $r_0 = 0.25, 0.5, \text{ and } 0.7 \mu\text{m}$ , and  $\sigma = 2$ , and the refractive indices for "Sahara dust-Barbados". Increasing  $r_0$  results in a small increase of single scattering albedo and asymmetry factor, and a large increase of extinction coefficient at infrared wavelengths, while the shape of the spectra remains almost unchanged. Similar changes in optical properties were found for all dust samples from Table 1.

We also analyzed the effect of a coarse mode of particles on the dust optical properties. The coarse mode has been observed in many experimental studies conducted near dust sources [D'Almeida, 1987]. Mineralogical composition of coarse mode particles is often almost 100% pure quartz [Gomes and Gillette, 1993]. Approximation of a coarse particle size spectrum by a lognormal function gives  $r_0$  in a range from 1 to 6  $\mu\text{m}$  [Levin and

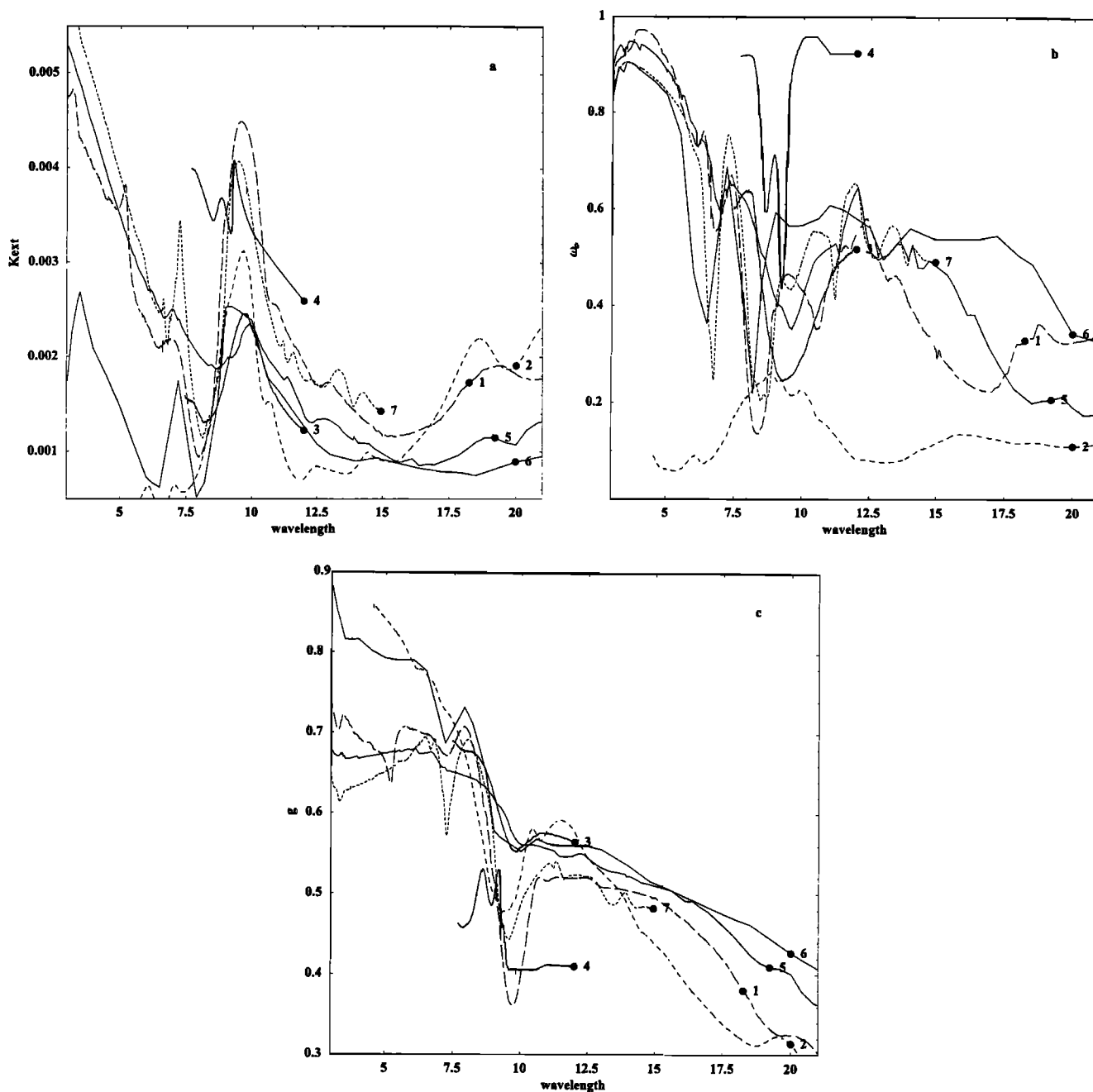


**Figure 2.** The (a) normalized extinction coefficients,  $K_{ext}$ , (b) single scattering albedo,  $\omega_0$ , and (c) asymmetry factor,  $g$ , for various complex refractive indices calculated for a lognormal size distribution with  $r_0 = 0.5 \mu\text{m}$ . Curve numbers are as in Figure 1.

Lindberg, 1979]. A common practice in modeling optical properties of dust in the coarse mode is to use the same refractive indices as for the accumulation mode. To test the adequacy of this approach, we calculated the coarse mode dust optical properties using refractive indices of amorphous quartz, and compared them to those calculated by using the refractive indices from Table 1. For amorphous quartz we used refractive indices published by Popova *et al.* [1972] which are in a good agreement with other published data.

Figures 4a and 4b present  $K_{ext}$  (normalized to  $N = 1 \text{ cm}^{-3}$ ) and  $\omega_0$  calculated assuming  $r_0 = 4 \mu\text{m}$ , as was recommended by D'Almeida *et al.* [1991] for the coarse mode of the dust particle

spectrum. As one can see in Figure 4, the largest differences between  $K_{ext}$  calculated with quartz refractive indices and with those from Table 1 are in the region 6 - 11  $\mu\text{m}$ , while discrepancies in  $\omega_0$  occur at all infrared wavelengths.

Analysis of the measurements of dust particle size distributions shows that typically there are two (or three) modes in the dust size spectra near dust source regions under high wind conditions, and there is only one mode in size spectra of dust particles which have been transported far from the source [Duce, 1994]. Therefore, dust optical properties will vary during the transport. It is common to explain the time-varying optical properties as a result of transformation of particle size distribution only, ignoring

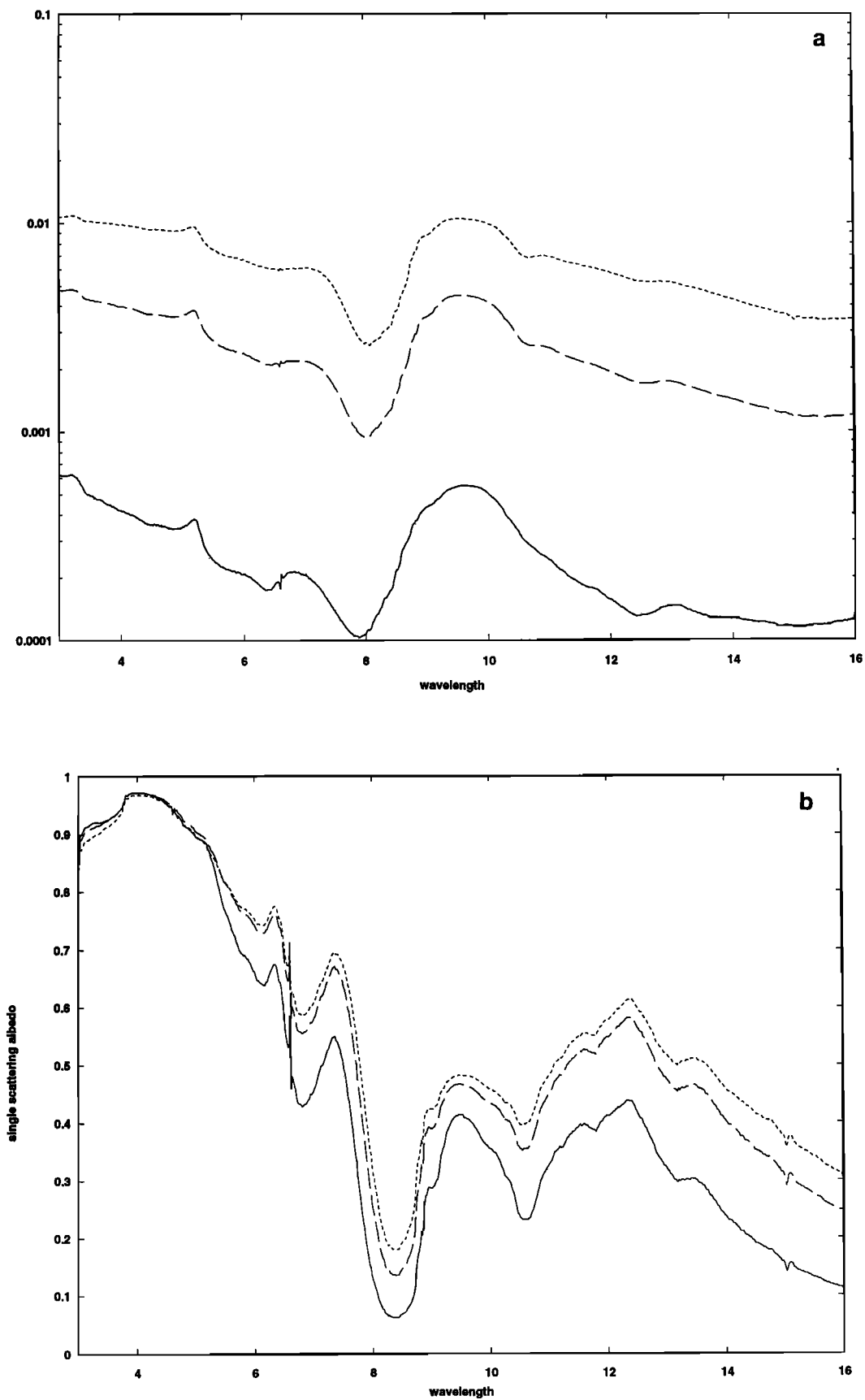


**Figure 3.** Spectra of (a) normalized extinction coefficients,  $K_{\text{ext}}$ , and (b) single scattering albedo,  $\omega_0$ , calculated for log-normal size distribution with  $r_0 = 0.25$  (solid lines),  $0.5$  (long dashed lines), and  $0.7$   $\mu\text{m}$  (short-dashed lines) for “Sahara dust-Barbados”.

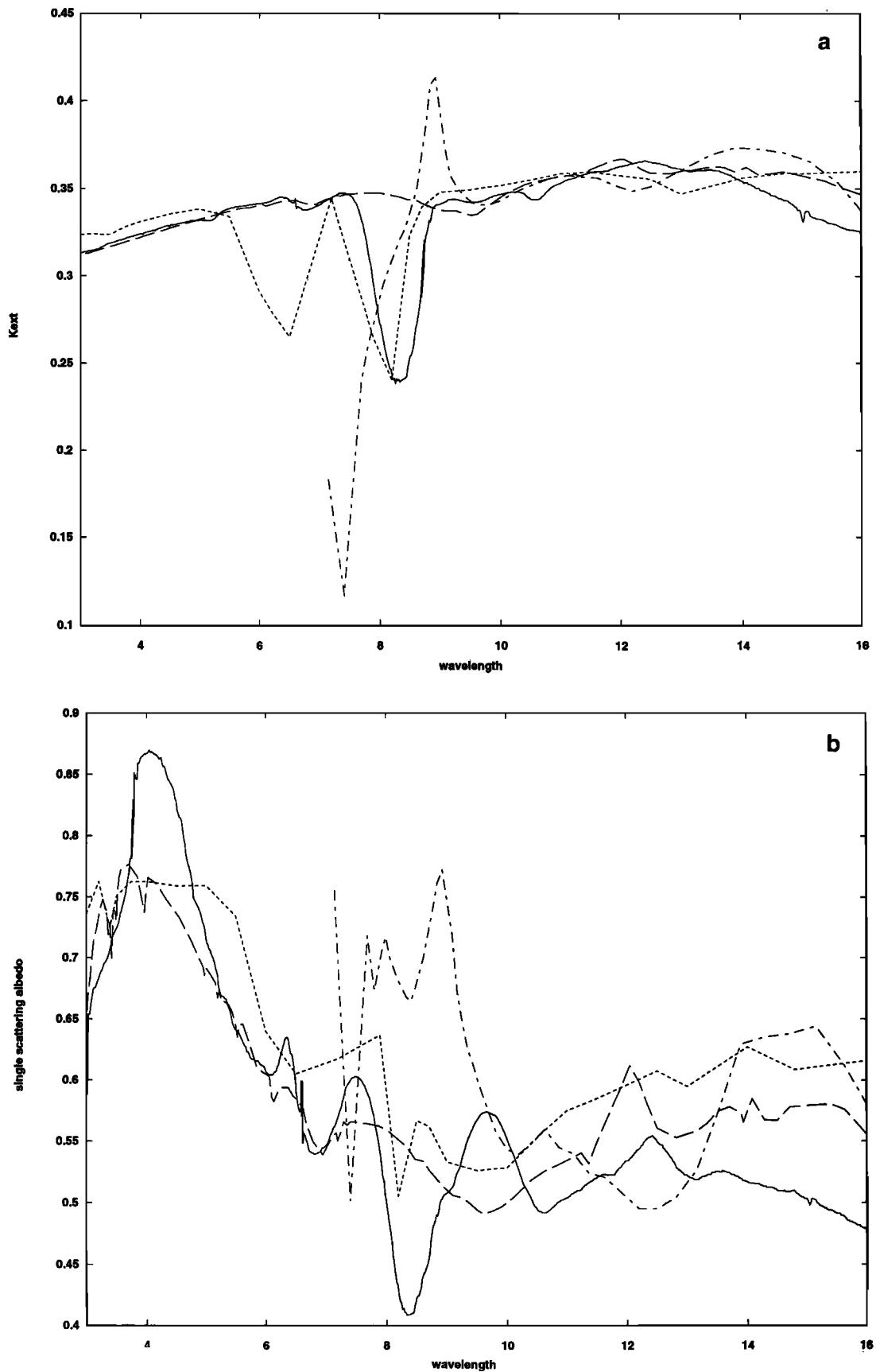


**Figure 4.** Spectra of (a) normalized extinction coefficient,  $K_{ext}$ , and (b) single scattering albedo,  $\omega_0$ , calculated for a lognormal size distribution with  $r_0 = 4 \mu\text{m}$  using refractive indices of amorphous quartz (dot-dashed line), “dust-like” (short-dashed line), “Afghan dust” (long-dashed line), and “Sahara dust-Barbados” (solid line).

the fact that varying mineralogical composition and, consequently optical constants, can alter the dust optical properties as well. The variations of mineralogical composition have been documented by numerous studies [e.g., *Pye*, 1987].

To illustrate the importance of time-varying mineralogical composition during the dust transport, we calculated the effective optical properties of airborne mineral aerosols having two modes in their size spectrum. We allowed the ratio of particle number concentrations in the coarse mode,  $N_c$ , to the concentration in the accumulation mode,  $N_a$ , to vary. The ratio  $N_c / N_a$  varies from 0 when the coarse mode is absent to about 1-2 when coarse mode particles are abundant (typically near the dust source under strong wind conditions [*Pye*, 1987]).

In particular, we calculated the effective single scattering albedo,  $\omega_{\text{eff}}$ , and the effective extinction coefficients,  $K_{\text{eff}}$  (normalized to  $N = 1 \text{ cm}^{-3}$ ) at three wavelengths 8.5, 11, and 12  $\mu\text{m}$  as a function of  $N_c / N_a$ . We selected these wavelengths because they are commonly used for satellite infrared observations [*Ackerman*, 1997]. We considered two cases of possible refractive indices for the accumulation and coarse modes. In the first case we calculated effective optical characteristics assuming that the accumulation mode has the refractive index of "Afghan dust" or "Sahara dust-Barbados", while the coarse mode has optical constants of amorphous quartz. In the second case we used refractive indices of "Afghan dust" or "Sahara dust-Barbados" for both accumulation and coarse modes. The effective optical characteristics were calculated in the following manner:

$$K_{\text{eff}} = (K_a N_a + K_c N_c) / (N_a + N_c),$$

$$\omega_{\text{eff}} = (\omega_a K_a N_a + \omega_c K_c N_c) / (K_a N_a + K_c N_c),$$

where  $K_a$  and  $K_c$  are the normalized extinction coefficients, and  $\omega_a$  and  $\omega_c$  are the single scattering albedos of the accumulation and coarse modes, respectively.

Figures 5a-5d present  $\omega_{\text{eff}}$  versus  $N_c / N_a$  for the combinations of refractive indices of the accumulation and coarse modes: Figure 5a is the case when "Afghan dust" refractive indices are used for the accumulation mode and amorphous quartz refractive indices are used for the coarse mode; Figure 5b is the case when both accumulation and coarse modes have refractive indices of "Afghan dust"; Figures 5c and 5d are the same as Figures 5a and 5b, except "Sahara dust-Barbados" refractive indices are used instead of "Afghan dust" refractive indices.

Figure 5 reveals many differences in the behavior of  $\omega_{\text{eff}}$  versus  $N_c / N_a$  for the combinations of refractive indices considered. For instance, when "Afghan dust" refractive indices are used for both size modes,  $\omega_{\text{eff}}$  calculated at 8.5 and 11  $\mu\text{m}$  are independent of  $N_c / N_a$ , while  $\omega_{\text{eff}}$  calculated at 12  $\mu\text{m}$  slightly decreases as  $N_c / N_a$  increases (see Figure 5b). In contrast, when amorphous quartz refractive indices are used for the coarse mode, the calculated  $\omega_{\text{eff}}$  at 11  $\mu\text{m}$  remains independent of  $N_c / N_a$ , while  $\omega_{\text{eff}}$  at 8.5  $\mu\text{m}$  monotonically increases and  $\omega_{\text{eff}}$  at 12  $\mu\text{m}$  decreases as  $N_c / N_a$  increases (see Figure 5a). Different behaviors of  $\omega_{\text{eff}}$  are observed for the case when "Sahara dust-Barbados" refractive indices are used (see Figures 5c and 5d). In this case,  $\omega_{\text{eff}}$  at 11 and 12  $\mu\text{m}$  show weak dependence on  $N_c / N_a$ , while  $\omega_{\text{eff}}$  at 8.5  $\mu\text{m}$  shows a drastic drop in magnitude when the accumulation and coarse modes have the same refractive indices as those of "Sahara dust-Barbados".

Figure 6 shows the change in effective normalized extinction coefficients that occurs when the coarse mode is treated as quartz

versus  $N_c / N_a$ . Figure 6a presents  $dK_{\text{eff}}$  calculated as  $K_{\text{eff}}$  for a case when the accumulation and coarse modes have the refractive index of "Afghan dust", minus  $K_{\text{eff}}$  for a case when the coarse mode has amorphous quartz refractive indices. Figure 6b is similar to Figure 6a, except the refractive index of "Sahara dust-Barbados" is used instead of "Afghan dust". One can see that magnitude of the differences in  $K_{\text{eff}}$  increases as  $N_c / N_a$  increases. The calculated differences in  $K_{\text{eff}}$  are important because their magnitudes are large enough to introduce errors into assessments of dust optical depth. For instance, if "Sahara dust-Barbados" refractive indices were used for both accumulation and coarse modes, one calculates an optical depth at 8.5  $\mu\text{m}$  of about 0.5 for  $N_c / N_a = 1 \times 10^{-2}$ , assuming that the total particle number concentration is  $100 \text{ cm}^{-3}$ . In turn, if the amorphous quartz refractive index is used for the coarse mode, one estimates an optical depth of 0.4. Therefore, an error in assessment of dust optical depth of about 0.1 can be introduced.

The cases considered above are rather simplified examples of possible varying mineralogical composition. However, our modeling of dust optical properties for varying refractive indices gave a large range of results, demonstrating the importance of incorporation of mineralogical composition into the dust life cycle to correctly calculate the time- and space-varying optical properties.

#### 4. Regional Dust Radiative Effects at Infrared Wavelengths

Based on our dust optical modeling and empirical data on dust loadings, we have simulated the profiles of downwelling and upwelling radiative fluxes at various geographical locations under various cloudless atmospheric conditions. To perform these calculations, we used an one-dimensional radiative transfer code, based on the correlated K distribution technique incorporated into a two-stream model [*Bergstrom et al.*, 1996; *Mlawer et al.*, 1997]. This code allows us to compute IR fluxes for arbitrary atmospheric conditions accounting for gaseous absorption along with absorption and scattering by atmospheric aerosols. *Mlawer et al.* [1997] show that the K distribution gives integrated flux results that are within  $1 \text{ W/m}^2$  of the line by line code. This result does not include the effects of aerosols or clouds.

The code has 16 bands in the infrared at the following wavelengths: 2600-3000, 2380-2600, 2250-2380, 2080-2250, 1800-2080, 1480-1800, 1390-1480, 1180-1390, 1080-1180, 980-1080, 820-980, 700-820, 630-700, 500-630, 250-500, and 10-250  $\text{cm}^{-1}$ . These bands have been selected to account for absorption by gases, ignoring aerosol absorption. Due to the specific structure in the spectra of dust optical characteristics (see Figure 2) a problem arises in correctly selecting dust optical characteristics for each wavelength band. To perform radiative transfer simulations, we calculated a weighted value of the optical characteristic,  $A_i$ , for each band as

$$A_i = \Sigma (A \delta\lambda) / \Sigma \delta\lambda,$$

where  $A$  is a given spectral optical characteristic (extinction coefficient, single scattering albedo, or asymmetry factor).

We selected several dust loading scenarios. We considered a "low dust loading" scenario to be representative for background conditions over arid or semiarid regions. The dust vertical profile was homogeneous in the lowest 4 km with  $N = 10 \text{ cm}^{-3}$  in each kilometer. For a case of "high dust loading" scenario the dust concentration was  $N = 100 \text{ cm}^{-3}$  [*D'Almeida*, 1987].

Dust vertical profiles can have a more complicated dependence

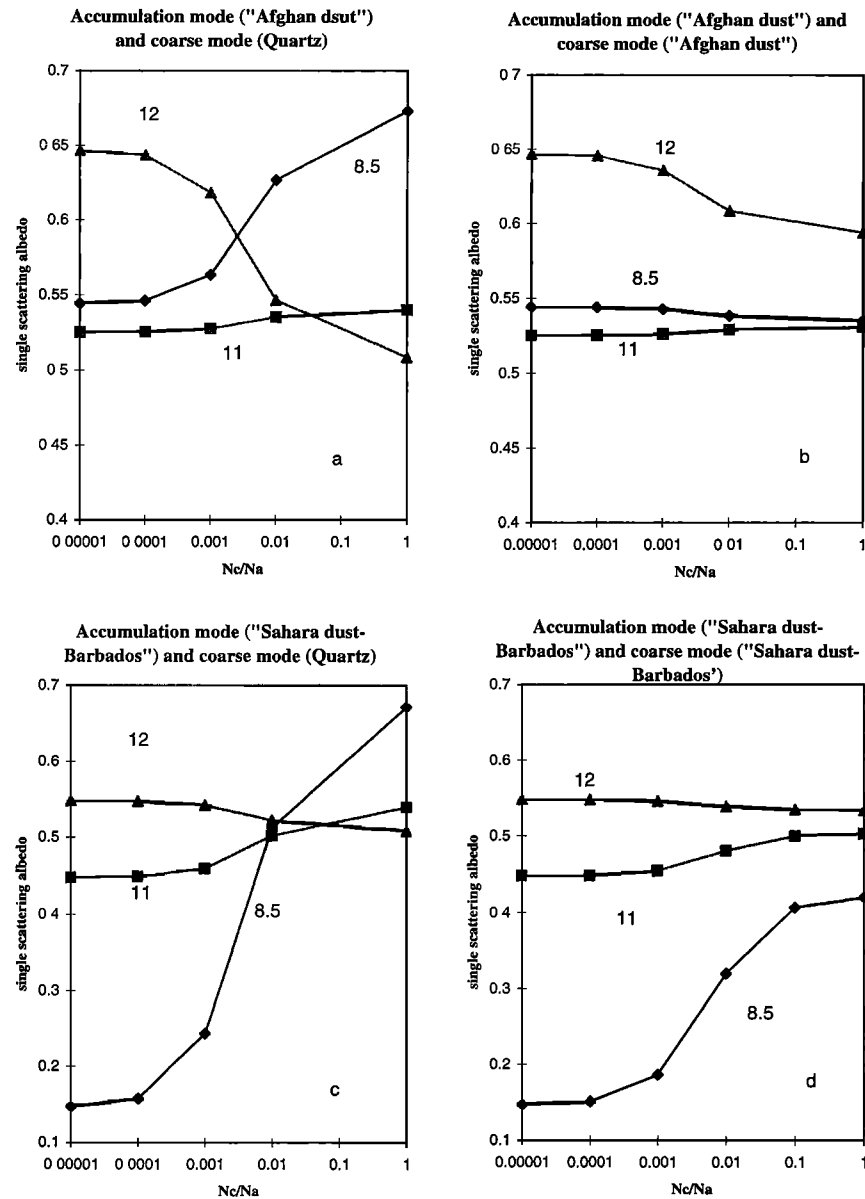


**Figure 5.** The effective single scattering albedo,  $\omega_{\text{eff}}$ , at three wavelengths 8.5, 11, and 12  $\mu\text{m}$  as a function of the ratio of particle number concentrations in the coarse mode and in the accumulation mode,  $N_c/N_a$  (see text for details).

on dust transport processes. Therefore, dust vertical distribution can vary in space and time. Our previous studies [e.g., Sokolik and Golitsyn, 1993] along with others demonstrated that variation of dust vertical distributions is more crucial for calculations of radiative heating/cooling rates in the dust layer than for IR fluxes at the surface, or at the top of the atmosphere which are a subject of the present paper. One can expect that an elevated dust layer will cause larger IR forcing than a dust layer near the surface, with the magnitude depending on the height of the layer and atmospheric conditions (temperature profile, water vapor profile, etc.). A detailed analysis of the importance of variation of dust vertical distribution for assessment of dust radiative effects is beyond the scope of the present paper, and it is a subject of our current research [Quijano et al., 1997]. Therefore, we limit our

modeling here to one type of dust vertical distribution which is representative for a well-mixed dust layer.

First, we modeled IR radiative effects for varying dust optical properties (see Figure 2) under "dry tropics" atmospheric conditions, which are representative of those for arid and semi-arid regions. The "dry tropics" model has the same vertical characteristics as a tropical standard atmosphere except the water vapor mixing ratio is lower (2.4 g/kg in the lowest 4 km). Figure 7 shows the changes relative to dust free conditions in IR downward fluxes at the surface,  $\Delta F_s$ , under "dry tropics" atmospheric conditions for the "low dust loading" and "high dust loading" scenarios calculated for the dust optical models from Figure 2. In all cases the additional loading of dust results in increasing IR downward fluxes at the surface; however, the

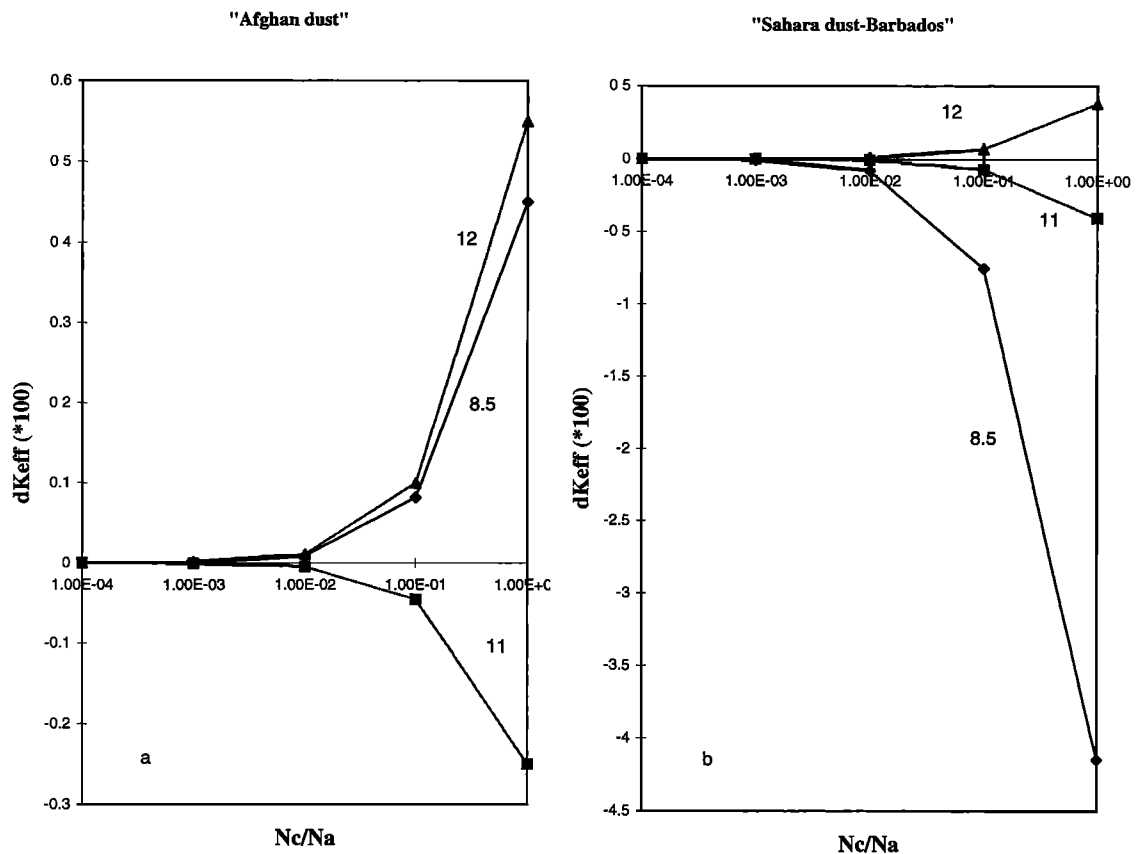


**Figure 6.** The differences in the effective normalized extinction coefficients,  $dK_{eff}$ , at three wavelengths 8.5  $\mu\text{m}$  (diamonds), 11  $\mu\text{m}$  (squares), and 12  $\mu\text{m}$  (triangles) as a function of the ratio of particle number concentrations in the coarse mode and in the accumulation mode,  $N_c/N_a$  (see text for details).

magnitudes vary for various dust optical models. For the “low dust loading” scenario the IR downward flux changes at the surface are in the range from 7 to 14  $\text{W}/\text{m}^2$ . In turn, for the “high dust loading” scenario the calculated  $\Delta F_s$  vary from 50 to 80  $\text{W}/\text{m}^2$ .

Figures 8a and 8b present calculated IR radiative forcing,  $\Delta F$ , at the top of the atmosphere for the low and high dust loading scenarios, respectively. The “low dust loading” caused an IR radiative forcing in the range from 2.2  $\text{W}/\text{m}^2$  to 6.5  $\text{W}/\text{m}^2$ , while for “high dust loading” it is in the range from 15  $\text{W}/\text{m}^2$  to 40  $\text{W}/\text{m}^2$ . These forcings greatly exceed those due to other atmospheric aerosols at infrared wavelengths.

Figures 7 and 8 present results for “dry tropics” atmospheric conditions. It is known that IR radiative effects of airborne mineral aerosols can strongly depend on atmospheric meteorological conditions (in particular, on water vapor and temperature profiles). While dust originates mainly in hot, dry regions, it can be transported over long distances to locations with different climates. To estimate the importance of varying dust optical properties on the IR radiative fluxes at various geographical zones and seasons, we performed calculations of  $\Delta F_s$  and  $\Delta F$  for several models of the standard atmosphere: midlatitude winter, midlatitude summer, sub-Arctic summer, and tropics.

Figures 9a and 9b shows the calculated variations of  $\Delta F_s$  and  $\Delta F$  for various atmospheric conditions, for the “low dust loading” scenario, and for two dust models: “Sahara dust-Barbados” and

“dust-like”. As one can see in Figure 9,  $\Delta F_s$  and  $\Delta F$  calculated for “Sahara dust-Barbados” are about twice as large as those calculated for “dust-like”. Both dust optical models produce larger IR effects under “dry tropics” atmospheric conditions than for other conditions.

Overall, our calculations demonstrate that the radiative effects of airborne mineral aerosols at infrared wavelengths are similar to those of “greenhouse” gases, but their magnitudes strongly depend on varying dust properties.

## 5. Discussion

The results presented above demonstrate that accounting for dust composition is required to decrease the currently large uncertainties in the assessment of IR radiative forcing by airborne mineral aerosols. One of the major problems is how to correctly account for varying dust composition for modeling dust radiative effects with regional or general circulation climate models. Recent studies on the global and regional modeling of dust aerosols considered time-variable size distributions but were limited to only one given spectrum of refractive indices. For instance, *Tegen and Fung* [1994] developed a transport model which describes sources, transport, and deposition of size-resolved mineral aerosols. The model has eight size bins to represent dust particles with radii  $0.1 \mu\text{m} < r < 10 \mu\text{m}$ . Each size class is treated as a separate tracer. However, Tegen and Fung employed the “Sahara dust-Barbados” (see Table 1) refractive

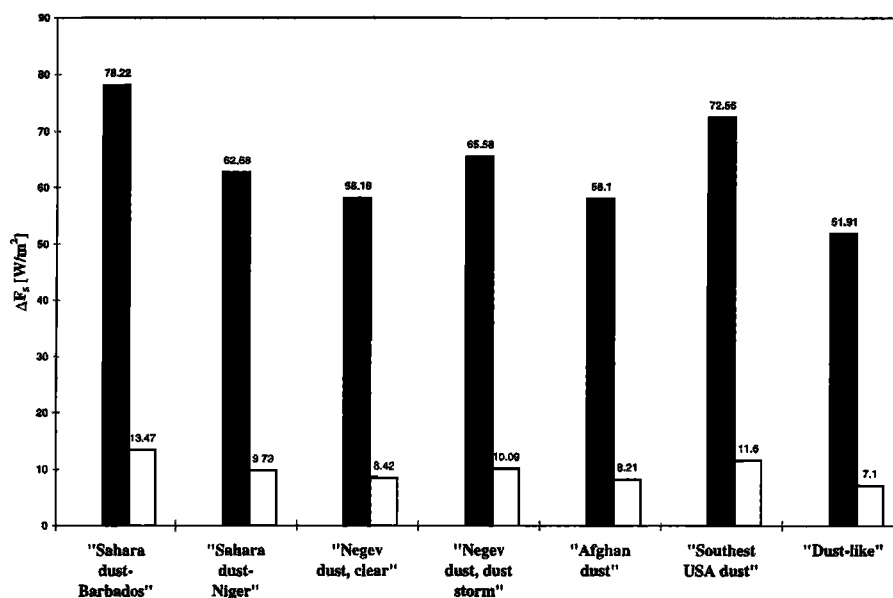


**Figure 7.** The changes in the IR downwelling fluxes at the surface,  $\Delta F_s$ , under “dry tropics” atmospheric conditions for the “low” (open bars) and “high” dust loading (solid bars) scenarios calculated for the dust optical models from Figure 2.

index to model global and regional dust radiative forcing, ignoring varying regional composition of dust and, therefore, varying dust optical constants. The calculations presented above indicate that using one spectrum of the refractive index could result in underestimation or overestimation of dust IR forcing at various regions with varying dust composition. For instance, Tegen and Fung’s model simulations will give a much larger IR forcing over western Europe compared to that which we calculate using “dust-like” refractive indices which may be more suitable for this region. Airborne mineral aerosols from specific regions will eventually need to be treated as the separate tracers.

Unfortunately, the available data for dust optical constants are very limited (see Table 1) and rather poor in quality. There is a strong need to develop a new data set of refractive indices and related dust composition for various dust source regions.

As we pointed out in section 2, one might prefer to model the major mineral constituents of the airborne dust aerosols, instead of using refractive indices for a mixture. Currently, we are working on defining the major components of mineral aerosols which should be taken into consideration to correctly represent spectral dust optical properties over a wide range of wavelengths from 0.2 to 30  $\mu\text{m}$ . For this purpose we are combining a data set of spectral refractive indices of various minerals, and performing modeling of the dust radiative properties utilizing available measurements of mineralogical compositions of airborne dust over various geographical regions. The results will be presented in a forthcoming paper.

Incorporation of such an approach into climate models will require information on production rates and time-dependent size distributions for each mineral considered. Existing global data sets of soil properties currently include soil texture (three size classes: “clay”, “silt” and “sand”) and soil types with resolution  $1^{\circ}\times 1^{\circ}$ , but they do not provide information on size-resolved mineralogical composition of the parent soil which can be transported by wind [Webb *et al.*, 1991]. Therefore, a new data set should be developed to provide necessary data for dust modeling on global and regional scales.

Furthermore, while the airborne dust composition also depends on mobilization processes, it is important to develop a parameterization to link mineralogical composition of parent soils to the size-resolved composition of the airborne dust. In turn, studies of dust emission show that the type of surface is important for the assessments of emitted dust. In particular, the ratio of clays to quartz is an important factor in fine dust production [Gillette, 1979, Marticorena and Bergametti, 1995].

Varying regional mineralogical and optical properties of airborne dust also can be a crucial factor in interpretation of the satellite infrared observations. Recent studies by Ackerman [1997] show that there are inconsistencies between theoretical simulations of the infrared properties of dust and satellite observations. The dust models used in that study are defined by a given size distribution and given refractive index [Longtin *et al.*, 1988]. Therefore, one of the possible reasons for discrepancies between simulations and observations is that the model considered did not link optical properties to time- and space-varying size distributions or mineralogical composition.

Incorporation of the mineralogical composition of the aerosols into climate models can also be beneficial for atmospheric chemistry modeling. There is growing evidence that chemical reactions on airborne mineral aerosol surfaces play an important role in the tropospheric chemistry of  $\text{SO}_x$ ,  $\text{NO}_y$ , and  $\text{O}_3$  [Dentener *et al.*, 1996]. To model the related chemical reactions, the size-resolved mineralogical composition of dust is required. For instance, the removal of  $\text{SO}_2$  and  $\text{HNO}_3$  depends on the alkalinity of dust aerosols; therefore, the calcium content should be known. Hydrogen radicals like  $\text{HO}_2$  and  $\text{OH}$  react on atmospheric particles through pathways involving redox reactions with iron; consequently the abundance of  $\text{Fe}^{3+}$  should be provided.

The successful accomplishment of the tasks discussed above will require a great deal of effort in acquiring new data sets as well as a better understanding of related physical processes. However, we can make some recommendations to improve the modeling of the radiative properties of airborne mineral aerosols using currently available data:

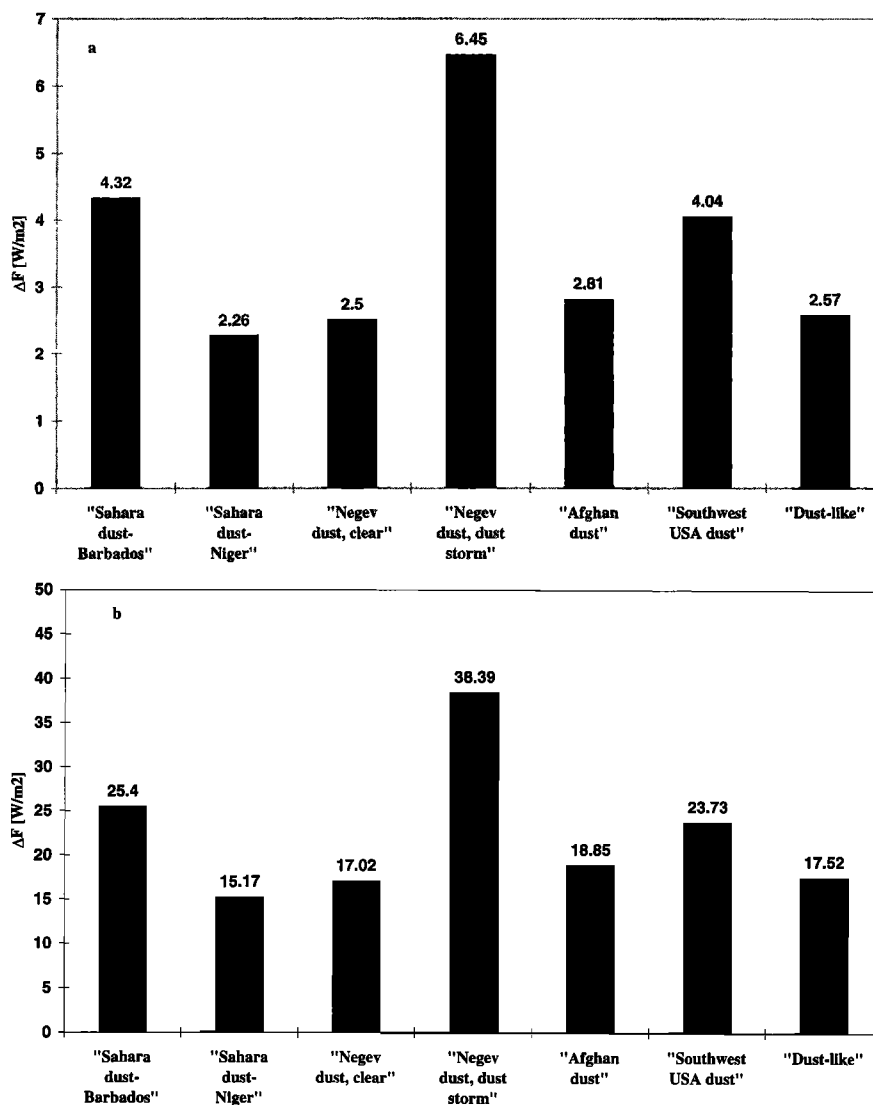


**Figure 8.** The IR radiative forcing at the top of the atmosphere,  $\Delta F$ , for the (a) "low" and (b) "high" dust loading scenarios calculated for the dust optical models from Figure 2.

1. Distinguish between desert dust and nondesert mineral aerosols generated from soils. For mineral aerosols of non-desert origin, use refractive indices of "dust-like" aerosols (see Table 1 and Figure 1).

2. Use refractive indices of "Sahara dust-Barbados", "Afghan dust", and "southwest USA dust" to model optical properties of long-living airborne dust in related geographical regions (see Table 1). For instance, use "Sahara dust-Barbados" refractive indices for the long-traveled, long-lived accumulation mode of dust particles (when the amount of quartz is about 10-15% by mass) which originates from the Sahara desert.

3. Near the dust source and under high wind conditions a coarse mode of dust particles with the refractive indices of quartz should be considered.

4. If the time-dependent dust particle size distributions for individual constituents are available, use optical constants of the individual constituents (see Table 2) to calculate the optical characteristics, and then calculate optical properties of the mixture to model varying dust optical properties.

## 6. Summary

In this paper we demonstrated the importance of the varying composition of airborne mineral aerosols for an assessment of

their regional direct radiative forcing at infrared wavelengths. We reexamined the available data on complex refractive indices of the mineral aerosols collected at various geographical locations. There is a great deal of variation in the values of the imaginary and real parts of the refractive index, which could be related to varying mineralogical compositions. Using spectral refractive indices, we performed calculations of the aerosol optical characteristics by employing Mie theory. We showed that the existing variations in refractive indices can cause large variations in the dust optical characteristics.

We calculated the IR radiative forcings and the IR downward fluxes at the surface, using our dust optics modeling, and empirical data on dust size distributions and dust loadings. The simulations performed gave a wide range of results for varying optical models of the mineral aerosols under the atmospheric conditions considered. Under "dry tropics" atmospheric conditions for the "low dust loading" scenario we estimated that for different dust optical models the changes in IR downward flux at the surface ("dust" minus "clean" conditions) are in the range from 7 to 14  $W/m^2$ , and the IR forcing is in the range from 2 to 7  $W/m^2$ . In turn, for the "high dust loading" scenario the calculated changes in IR flux at the surface are in the range from 50 to 80  $W/m^2$ , and the IR forcing is in the range from 15 to 25  $W/m^2$  for varying optical models. The magnitudes of the changes in the IR

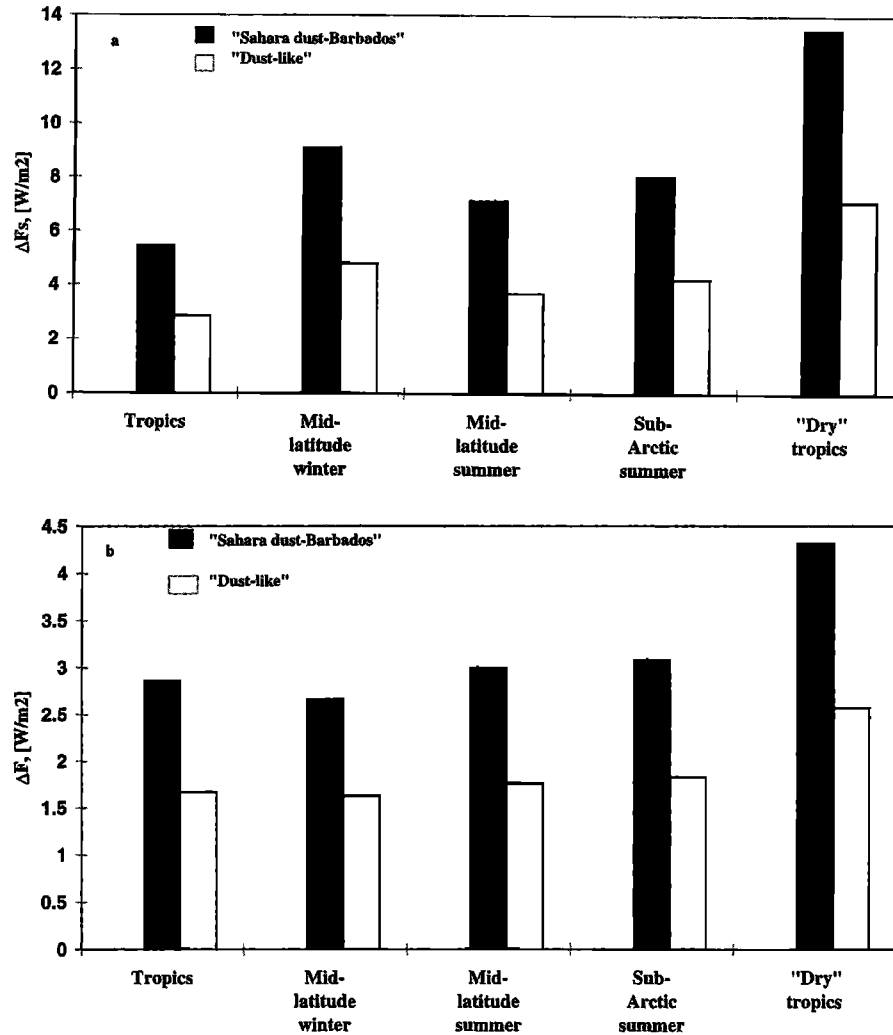


**Figure 9.** Calculated (a)  $\Delta F_3$  and (b)  $\Delta F$  for different atmospheric conditions for two dust models, "Sahara dust-Barbados" and "dust-like", under the "low" dust loading scenario.

fluxes and the IR forcing for "dry tropics" atmosphere are higher than those calculated for other atmospheric conditions: midlatitude winter, midlatitude summer, sub-Arctic Summer, and tropics.

We conclude that incorporation of regionally and temporally varying dust mineralogical composition into GCM and regional models could be beneficial for decreasing the currently large uncertainties in assessments of radiative forcing by the natural and anthropogenic components of the airborne mineral aerosols. Treatment of variable dust composition can be crucial for remote sensing of the atmospheric aerosols using satellite infrared observations. Information on mineralogical composition could also be helpful for atmospheric chemistry modeling.

**Acknowledgments.** This research was supported by NASA-Ames grant NAG2-1116; NASA EOS-IDS grant NAG 5-6504; and ONR grant N00014-98-1-0121. The authors would like to thank Eli Mlawer and Tony Clough of Atmospheric and Environmental Research, Inc., for providing the K distributions used in this study.

## References

Ackerman, S., Remote sensing aerosols using satellite infrared

- observations, *J. Geophys. Res.*, *102*, 17069-17079, 1997.
- Aronson, J. R., A. G. Emslie, E. V. Mises, E. M. Smith, and P. F. Strong, Optical constants of monoclinic anisotropic crystals: Gypsum, *Appl. Opt.*, *22*, 4093-4098, 1983.
- Bergstrom, R.W., Comments on the estimation of the absorption coefficients of atmospheric aerosols, *Cont. Atmos. Phys.*, *46*, 223-231, 1973.
- Bergstrom, R.W., S. Kinne, I. N. Sokolik, O. B. Toon, E. Mlawer, A. Clough, and T. Ackerman, 3ARM: A fast, accurate radiative transfer model for use in climate studies, paper presented at International Radiation Symposium, Am. Meteorol. Soc., Fairbanks, Alaska, Aug. 19-24, 1996.
- Carlson, T.N., and S. Benjamin, Radiative heating rates for Sahara dust, *J. Atmos. Sci.*, *37*, 193-213, 1980.
- D'Almeida, G. A., On the variability of desert aerosol radiative characteristics, *J. Geophys. Res.*, *92*, 3017-3026, 1987.
- D'Almeida, G. A., P. Koepke, and E. P. Shettle, *Atmospheric Aerosols: Global Climatology and Radiative Characteristics*. A. Deepak, Hampton, Va., 561pp., 1991.
- Dentener, F., G. Carmichael, Y. Zhang, P. Grutsen, and J. Leliefeld, The role of mineral aerosols as a reactive surface in

- the global troposphere *J. Geophys. Res.*, *101*, 22869-22890, 1996.
- Duce, R.A., Sources, Distributions, and fluxes of mineral aerosols and their relationship to climate, in *Aerosol Forcing of Climate*, edited by R. J. Charlson and J. Heintzenberg, pp. 43 - 72, John Wiley, New York, 1994.
- Fisher, K., The optical constants of atmospheric aerosol particles in the 7.5 - 12  $\mu\text{m}$  spectral region, *Tellus*, *XXVIII*, 266 - 274, 1976.
- Fouquart, Y., B. Bonnel, G. Brogniez, J.C. Buriez, L. Smith, J.J. Mockette, and A. Cerf, Observations of Saharan aerosols: Results of ECLATS field experiment, II, Broadband radiative characteristics of the aerosols and vertical radiative flux divergence, *J. Clim. and Appl. Meteorol.*, *26*, 38-52, 1987.
- Gillette, D. A., Environmental factors affecting dust emission by wind erosion, in *Sahara Dust*, Edited by C. Morales, pp.71-94, John Wiley, New York, 1979.
- Glassum, R.A., and J.M. Prospero, Saharan aerosols over the tropical North Atlantic: Mineralogy, *Mar. Geol.*, *37*, 295-321, 1980.
- Gomes, L., and D. A. Gillette, A comparison of characteristics of aerosol from dust storms in central Asia with soil-derived dust from other regions. *Atmos. Environ.*, *27A*, 2539-2544, 1993.
- Levin, Z., and J. D. Lindberg, Size distribution, chemical composition and optical properties of urban and desert aerosols in Israel, *J. Geophys. Res.*, *84*, 6941-6950, 1979.
- Long, L. L., M. R. Querry, R. J. Bell, and R. W. Alexander, Optical properties of calcite and gypsum in crystalline and powdered form in the infrared and far-infrared, *IR Phys.*, *34*, 191-201, 1993.
- Longtin, E.R., E.P. Shettle, J.R. Hummel, and J.D. Pryce, A wind dependent desert aerosol model: Radiative properties, AFGL-TR - 88 - 0112, 105 pp., Air Force Geophys. Lab., Air Force Syst. Command, Hanscom Air Force Base, Mass., 1988.
- Martcorena, B., and G. Bergametti, Modeling the atmospheric dust cycle, 1, Design of a soil-derived dust emission scheme, *J. Geophys. Res.*, *100*, 16415-16430, 1995.
- Mlawer, E.J., S. J. Taubman, P. D. Brown, M. J. Iacono and S. A. Clough, Radiative transfer for inhomogeneous atmospheres: RRTM, a validated correlated-k model for the longwave, *J. Geophys. Res.*, *102*, 16663-16682, 1997.
- Parungo, F., et al., Asian dust storms and their effects on radiation and climate, part 1, Rep. TR 2906, Sci. and Technol. Corp., Hampton, Va., 1995.
- Patterson, E. M., Optical properties of the crustal aerosol: Relation to chemical and physical characteristics, *J. Geophys. Res.*, *86*, 3236-3246, 1981.
- Patterson, E. M., and D. A. Gillette, Commonalities in measured size distributions for aerosols having a soil-derived component, *J. Geophys. Res.*, *82*, 2074-2082, 1977.
- Peterson, J. T., and J. A. Weinman, Optical properties of quartz dust particles at infrared wavelengths, *J. Geophys. Res.*, *74*, 6947-6952, 1969.
- Popova, S. I., T. S. Tolstykh, and V. T. Vorobev, Optical characteristics of amorphous quartz in the 1400 - 200  $\text{cm}^{-1}$  region, *Opt. Spectrosc.*, *33*, 444-445, 1972.
- Popova, S. I., T. S. Tolstykh, and L. S. Ivlev, Optical constants of  $\text{Fe}_2\text{O}_3$  in the infrared range of the spectrum, *Opt. Spectrosc.*, *35*, 551-552, 1973.
- Pye, K., *Aeolian Dust and Dust Deposits*, 334 pp., Academic, San Diego, Calif., 1987.
- Querry, M. R., Optical constants of minerals and other materials from the millimeter to the UV, Rep. CRDEC-CR-88009, U.S. Army, Aberdeen, MD, 1987.
- Querry, M. R., G. Osborne, K. Lies, R. Jordon, and R. Coveney, Complex refractive index of limestone in the visible and infrared, *Appl. Opt.*, *17*, 353-356, 1978.
- Quijano, A. L., I. N. Sokolik, and O. B. Toon., Modeling radiative heating rates due to airborne mineral aerosols. EOS Trans. AGU, Fall Meet., Suppl., F109, 1997.
- Roush, T., J. Pollack, and J. Orenberg, Derivation of midinfrared (5-25  $\mu\text{m}$ ) optical constants of some silicates and palagonite, *Icarus*, *94*, 191-208, 1991.
- Salisbury, J. W., L. S. Water, N. Vergo, and D. M. Dana, *Infrared (2.1-25  $\mu\text{m}$ ) Spectra of Minerals*, 267 pp., Johns Hopkins Univ. Press, Baltimore, Md., 1992.
- Sokolik, I. N., and G. Golitsyn, Investigation of optical and radiative properties of atmospheric dust aerosols, *Atmos. Environ.*, *27A*, 2509-2517, 1993.
- Sokolik, I. N., and O. B. Toon, Direct radiative forcing by anthropogenic mineral aerosols, *Nature*, *381*, 681-683, 1996a.
- Sokolik, I. N., and O. B. Toon, Direct radiative forcing by airborne mineral dust, *J. Aerosol Sci.*, *27*, Suppl. 1, S11, 1996b.
- Sokolik, I. N., A. V. Andronova, and T. C. Johnson, Complex refractive index of atmospheric dust aerosols, *Atmos. Environ.*, *27A*, 2495-2502, 1993.
- Sokolik, I. N., R. W. Bergstrom, and O. B. Toon, Modeling of optical and radiative characteristics of the airborne mineral aerosol in infrared region, paper presented at *Ninth Conference on Atmospheric Radiation*, Am. Meteorol. Soc., Long Beach, Calif., Feb. 2-7, 1997.
- Steyer, T.R., L. Day, and D. R. Huffman, Infrared absorption by small amorphous quartz sphere, *Appl. Opt.*, *13*, 1586-1590, 1974.
- Tegen, I., and I. Fung, Modeling of mineral dust in the atmosphere: Sources, transport, and optical thickness, *J. Geophys. Res.*, *99*, 22897-22914, 1994.
- Tegen, I., A. A. Lacis, and I. Fung, The influence on climate forcing of mineral aerosols from disturbed soils, *Nature*, *380*, 419-422, 1996.
- Toon, O.B., J. B. Pollack, and C. Sagan, Physical properties of the particles composing the Martian dust storm of 1971-1972, *Icarus*, *30*, 663-696, 1977.
- Volz, F. E., Infrared absorption by atmospheric aerosol substances, *Appl. Opt.*, *11*, 755-759, 1972.
- Volz, F. E., Infrared optical constant of ammonium sulfate, Sahara dust, volcanic pumice, and flash, *Appl. Opt.*, *12*, 564-658, 1973.
- WCP-55, *WMO Report of the Experts Meeting on Aerosols and Their Climatic Effects*, World Meteorol. Organ., 1983.
- Webb, R., C. Rosenzweig, and E. H. Levine, A global data set of particle size properties, *NASA Tech. Rep.*, *NASA TM-4286*, 33 pp., 1991.

R.W. Bergstrom, Bay Area Environmental Research Institute, 3430 Noreiga St., San Francisco, CA 94122. (e-mail: bergstro@arc.nasa.gov)  
 I.N. Sokolik and O.B. Toon, Atmospheric and Oceanic Sciences Department and Laboratory for Atmospheric and Space Physics, Campus Box 392, University of Colorado at Boulder, Boulder, CO 80309. (e-mail: sokolik@alcor.colorado.edu)